https://doi.org/10.5194/gi-2019-42
Preprint. Discussion started: 22 June 2020
© Author(s) 2020. CC BY 4.0 License.

Geoscientific Instrumentation Methods and Data Systems Discussions

Research on real-time elimination of UWB radar ranging abnormal value data

Xin Yan, Hui Liu, Guoxuan Xin, Hanbo Huang, Yuxi Jiang, Ziye Guo

School of Electrical and Information Engineering, Beijing University of Civil Engineering and Architecture. Beijing 100044, China

Correspondence to: Xin Yan(yx19941029@126.com)

Abstract. For indoor positioning, ultra-wideband (UWB) radar comes to the forefront due to its strong penetration, anti-jamming, and high precision ranging abilities. However, due to the complex indoor environment and disorder of obstacles, the problems of diffraction, penetration, and ranging instability caused by UWB radar signals also emerge. During the experiment of indoor positioning with UWB radar ranging module P440, it was found that the distance information measured in a short time was unstable, because of the complex indoor environment and unpredictable noise signal. Therefore, the abnormal value migration of the positioning trajectory occurred in real-time positioning. To eliminate this phenomenon and provide more accurate results, the abnormal values need to be removed. It is not difficult to eliminate abnormal value accurately based on a large number of data, but it is still a difficult problem to ensure the stability of the positioning system by using a small amount of measurement data in a short time to eliminate abnormal value in real-time ranging data. Thus, this paper focuses on the experimental analysis of a UWB-based indoor positioning system. To improve the stability of UWB radar ranging data and increase the overall accuracy, this paper studies a large number of UWB radar ranging data by using high-frequency ranging instead of mean value to train estimation model. Based on the Gaussian function outlier detection, abnormal values are eliminated. By using the training distance estimation model and estimating the distance value, the ranging error obtained is nearly 50% lower than the peak and mean ranging errors in general.

1 Introduction

UWB technology, due to its high transmission rate, penetration, security, and low system complexity, has been favored by many scholars in the field of indoor positioning. In 2014, Khajenasiri et al. (2014) developed a low power UWB transceiver for smart home energy consumption monitoring and management, which is one order lower than the commercial wireless technology applied in smart home applications. In 2017, Mokhtari et al. (2017) put forward the use of UWB technology to monitor some high-risk areas in a smart home environment. In 2012, Madany et al. (2012) investigated ITS and proposed the use of UWB technology in vehicle-to-vehicle and vehicle-to-infrastructure communication of multi-user ITS technology. In 2018, Mostajeran et al. (2018) proposed a UWB full-scale imaging radar with Asia-Pacific Hertz frequency. This was the

https://doi.org/10.5194/gi-2019-42
Preprint. Discussion started: 22 June 2020
© Author(s) 2020. CC BY 4.0 License.

Geoscientific Instrumentation Methods and Data Systems Discussions

first THz/sub-THz frequency imaging radar providing good lateral resolution without any focal lens or reflector. For objects with a distance of 23cm, it achieved 2mm lateral resolution and 2.7mm range resolution.

In 2016, Kim and Choi (2016) proposed an automatic landing system for UAS based on the UWB, optimized the geometric structure of the UWB anchor in the network, and achieved a more accurate positioning performance for the UAS landing process. In 2018, Nakamura et al. (2018) studied a pedestrian positioning system based on UWB ranging. In this system, the base station receiving the UWB signals transmitted by the pedestrians was connected to the traffic lights, and the locations of pedestrians was estimated by the least square method using the distance estimated by the UWB ranging scheme. In 2017, Kolakowski (2017) proposed the concept combining Bluetooth low power (BLE) and UWB positioning to improve the energy efficiency. In 2017, Ruiz et al. (2017) compared the performance of three commercial UWB systems, namely Ubisense, BeSpoon, and DecaWave, under the same experimental conditions. A measurement model combining Bayesian and particle filters was used. The model considered errors in distance measurement and found the abnormal values. The results indicated which system performed better under these industrial conditions. In 2015, Ledergerber et al. (2015) proposed a self-positioning robot system based on one-way UWB communication. By passively receiving the UWB radio signals from a fixed position, the position of the robot in a certain space was estimated. In 2016, Hepp et al. (2016) proposed an omnidirectional tracking system for flying robots based on blocking robust UWB signals. Compared to the typical UWB positioning systems with a fixed UWB converter in the environment, this system only needed one UWB converter to detect the target. In 2017, Perez-Grau et al. (2017) proposed a multi-modal mapping system based on UWB and RGB-D. By using the synergy between the UWB sensor and point cloud, a multi-mode three-dimensional (3D) map with a UWB sensor was generated for location estimation, which was integrated into the Monte Carlo localization method. In 2018, Schroeer (2018) used a real-time UWB multi-channel indoor positioning system for industrial scenes to evaluate multi-path and non-line-of-sight situations. In the same year, Stampa et al. (2018) proposed a semi-automatic calibration method for the UWB-based distance measurement of the autonomous mobile robots. Aiming at the system ranging error observed in the UWB distance measurement, a semi-automatic calibration method was proposed to estimate the error model approximating its influence.

The research on UWB in China, however, started relatively late. Although it is not as mature as that of foreign countries, some works have been done with the strong support of the state. In 2010, Chen et al. (2010) designed a UWB transmitter combined with a digital pulse generator and a modulator to minimize the power consumption. In 2015, Wang et al. (2015) proposed the use of UWB technology to monitor the load in football training. In 2016, Zhang et al. (2016) used UWB radar to image two targets behind the double-wall using the time-domain back projection (BP) and the frequency domain phase shift (PSM) algorithms. In 2017, Ke et al. (2017) proposed an integrated method of intelligent vehicle navigation and positioning based on GPS and UWB. When a vehicle was in a position where the GPS signals were difficult to receive, such as tunnels, the positioning was fulfilled by UWB, and the lost GPS signals were used to replace the integrated positioning of the vehicles. In 2016, Dai et al. (2016) analyzed the main factors affecting the UWB positioning accuracy in a hazardous chemicals warehouse and accordingly proposed a UWB four-reference vector compensation method for the stacking location,

https://doi.org/10.5194/gi-2019-42
Preprint. Discussion started: 22 June 2020
© Author(s) 2020. CC BY 4.0 License.

Geoscientific Instrumentation Methods and Data Systems Discussions

which was suitable for monitoring the five-segment distance. In 2017, Fu et al. (2017) proposed a method to detect the attitude of the road header by using the UWB ranging technology to realize the unmanned driving.

UWB radar is favored by researchers of indoor positioning systems because of its strong penetration, anti-jamming, and high precision ranging ability. However, due to the complex indoor environment and the disorder of obstacles, the problem of diffraction, penetration, and ranging instability of UWB radar signals also emerge. Thus, this paper focuses on the experimental analysis of a UWB-based indoor positioning system. To , the stability and accuracy of UWB radar ranging data are further improved. Aiming at the real-time measurement of a large amount of UWB radar ranging data, this paper proposes that the processing of the acquired data has to be performed immediately to meet the real-time requirement of the positioning systems. Thus, abnormal values and redundant data in ranging can be removed in real-time, and more accurate and stable results can be delivered to an indoor positioning module.

that the range information measured in a short time is very unstable and even has abnormal values due to the complex indoor environment and unpredictable noise signals. The abnormal values should be eliminated. Based on this, this paper focuses on the experimental analysis of a UWB radar indoor positioning system. To improve the stability of UWB radar ranging data and increase the overall accuracy, this paper studies a large number of UWB radar ranging data by using high-frequency ranging instead of mean value to train estimation model. The high-frequency range value is used instead of the mean value, and the distance estimation model is trained. The abnormal value is detected based on the function, and the abnormal value is removed after training. The ranging error obtained by distance measurement is nearly 50% lower than that of peak and mean ranging errors.

2 P440 UWB wireless sensor location framework

The P440 UWB wireless sensor operates at a center frequency of 4.3 GHz and has a bandwidth of 2.2 GHz. The signal ranging accuracy of ideal laboratory environment calibration can reach 0.05 m and works well in extremely challenging environments. The testbed for positioning in laboratory using the P440 UWB wireless sensor is shown in Fig. 1.

This experiment is used to realize indoor 3D positioning. Four P440 UWB wireless sensors are used as base stations (also called anchor nodes), and a P440 UWB wireless sensor is used as a node to be tested, which can be installed in mobile devices usually used in indoors (e.g., sports robots). The P440 can obtain the distance information between two nodes. By using this and the positioning algorithm, the t coordinates of each node in 3D can be acquired, and the three-dimensional positioning result of the node to be tested can be obtained.

The experimental results of the 3D positioning in a laboratory environment are shown in Fig. 2. It is found that, due to the complex indoor environment, the interference from indoor objects is relatively serious, resulting in unstable distance information measured in a short period of time, and even abnormal values. Therefore, when performing real-time positioning, the positioning trajectory generates an abnormal value offset phenomenon. In order to improve the stability and accuracy of

https://doi.org/10.5194/gi-2019-42
Preprint. Discussion started: 22 June 2020
© Author(s) 2020. CC BY 4.0 License.

Geoscientific Instrumentation Methods and Data Systems Discussions

the real-time positioning, the original ranging data need to be analysed and processed as reducing the influence of the abnormal values, so that the target point to be tested is stabilized in a small range.

3 Ranging data analysis

3.1 Distribution function and parameter estimation of the ranging data

In the laboratory environment, two P440 wireless sensors were used to obtain a large amount of ranging data from four different distance locations, and Fig. 3 shows the histogram of the data acquired. As seen, the data obtained follows a Gauss distribution, which can be formulated as

$$f(x) = \frac{1}{\sqrt{2\pi}\sigma} exp\left[-\frac{(x-\mu)^2}{2\sigma^2}\right] \quad (1)$$

The laboratory fits its probability density distribution curve for these four sets of data, as shown in Fig. 4. As seen, the expected value deviates from the true value, i.e., there is a huge difference in the standard deviation of the Gaussian distribution for each group of data. Table 1 gives the expected and standard deviation of the estimated four sets of data. This is an indicator of abnormal values, which causes measurement discrepancy between the measurements and the true values. Thus, the data cannot be used for positioning due to the abnormal values.

3.2 Mean, peak, and true values of the ranging data

In the above-given measurement data, due to the disturbance of abnormal values, the deviation between the expected, peak, and the true values are high. In positioning, especially for mobile tracking, it is impossible to collect a large amount of data in a short time. Therefore, we collected only 60 groups of measurement data from different distances and accordingly calculated their mean and peak values.

3.3 Distance estimation model training

Figure 5 and Table 2 show that using the mean peak as a reference, though and there is certain error between the true value, but it can be seen that the distance between true value and measure the peak of a certain linear relationship will be measured, as shown in Fig. 6 (scattered dots in red). By using a polynomial, 50 of the 60 sets of data were selected as the training set to fit the linear relationship between the peak and the true values of the measured data, as shown by the solid cyan line in Fig. 6. The other 10 sets are set aside as test sets. Table 2 shows the statistical results of the true, peak, and mean values of the selected 50 groups of data.

https://doi.org/10.5194/gi-2019-42
Preprint. Discussion started: 22 June 2020
© Author(s) 2020. CC BY 4.0 License.

Geoscientific Instrumentation Methods and Data Systems Discussions

4 Data processing methods

The statistical results of the peak and true values in Section 3 showed that the deviation between the peak and the true values is linear, satisfying a certain relationship. Since the ranging data follows a Gaussian distribution, the peak value is taken as the reference mean for processing. Then, the ranging results that the reference mean meets certain conditions are retained, and those that do not meet the conditions, i.e., abnormal values are removed. Finally, the true value of the distance is estimated for normal data according to the fitted curve in Fig. 6 reducing the ranging error. By using linear fitting, the relationship between the peak and true values can be formulated as

$$y = 0.9859x - 0.1633, \tag{2}$$

where x is the peak value, and y is the true.

4.1 Gaussian abnormal value detection

Since the distance measurement follows a Gaussian distribution $N\sim(\mu,\sigma^2)$, the Gaussian function is used for abnormal value detection. Here, the abnormal values and the normal data are calibrated, the abnormal value data is eliminated, and the normal data is retained.

$$x = (y + 0.1633)/0.9859. \tag{3}$$

Since the measurement data satisfies the Gaussian distribution $N\sim(\mu,\sigma^2)$, it is known from (3) that when the distance estimation is carried out by (2), the estimated value also satisfies the Gaussian distribution. The estimated mean μ_y the and standard deviation σ_y can be expressed as

$$\mu_y = 0.9859\mu - 0.1633, \tag{4}$$

$$\sigma_y = 0.9859\sigma. \tag{5}$$

Therefore, if it is desired to obtain an estimated value error less than δ_y, the error x between the measured value of δ_x and the peak value has to satisfy $\delta_x < \delta_y/0.9859$.

According to this method, abnormal values were detected for the four groups of data, and the results were shown in Fig. 7. As seen, the method successfully removes the abnormal values. Among the four groups of data, the first three groups had a very large standard deviation due to the existence of abnormal value. After the elimination of abnormal value, the standard deviation remained within 50mm.

4.2 Estimating the truth value

After removing the abnormal value by the Gaussian function, according to the above analysis, the ranging value cannot be directly used for positioning. This is because the error between the ranging peak and the true values of the P440 is still high,

https://doi.org/10.5194/gi-2019-42
Preprint. Discussion started: 22 June 2020
© Author(s) 2020. CC BY 4.0 License.

Geoscientific Instrumentation Methods and Data Systems Discussions

and thus the required ranging value needs to be retained. The estimation is performed by using (2), and the results are shown in Table 3, which gives the estimated values of the 10 sets of test data. Table 4, on the other hand, shows the overall error when estimating the ranging distance by using peaks, expected values, and the methods proposed in this paper.

5 Conclusion

In this paper, the experimental analysis and research on the ranging data of the UWB radar indoor positioning system were carried out. To meet the needs of indoor real-time positioning, further improve the stability of UWB radar ranging data and the overall accuracy, a large amount of UWB radar ranging data were studied, and the high-frequency ranging value was used to replace the mean value and train the range estimation model. The abnormal value was detected based on the Gaussian function. After removing the abnormal value, the distance estimation model was used to estimate the distance value. The results showed that the distance measurement error obtained is nearly 50% lower than the peak and mean distance measurement errors.

Author contribution

Xin Yan and BB designed the experiments and Xin Yan developed the model code. Xin Yan, Guoxuan Xin and Hanbo Huang carried them out. Xin Yan prepared the manuscript with contributions from all co-authors. Hui Liu, Yuxi Jiang and Ziye Guo revised the manuscript.

Competing interests

The authors declare that they have no conflict of interest.

Funding

Name of Funder: National Natural Science Foundation of China
Grant Agreement No.: 61501019
Name of Funder: Scientific Research Project of Beijing Educational Committee
Grant Agreement No.: SQKM201710016008
Name of Funder: The Fundamental Research Funds for Beijing University of Civil Engineering and Architecture
Grant Agreement No.: 18209

https://doi.org/10.5194/gi-2019-42
Preprint. Discussion started: 22 June 2020
© Author(s) 2020. CC BY 4.0 License.

Geoscientific Instrumentation Methods and Data Systems Discussions

References

Chen, F. H., Lin, S. Y., Li, L. Y., Sun, X. W.: 4.2-4.8 GHz CMOS variable gain LNA for Chinese UWB application, in: 2010 International Conference on Microwave and Millimeter Wave Technology, Chengdu, China, 8-11 May 2010, 1922-1924, 2010.

Dai, B., Lv, X., Liu, X. J., Li, Z. C.: A UWB-based four reference vectors compensation method applied on hazardous chemicals warehouse stacking positioning, CIESC J., 67, 871-877, 2016.

Fu, S., Li, Y., Zong, K., Zhang, M., Wu, M.: Accuracy analysis of UWB pose detection system for roadheader, Chin. J. Sci. Instrum., (8), 17, 2017. (in Chinese)

Hepp, B., Nägeli, T., Hilliges, O.: Omni-directional person tracking on a flying robot using occlusion-robust ultra-wideband signals, in: 2016 IEEE/RSJ International Conference on Intelligent Robots and Systems (IROS), Daejeon, South Korea, 9-14 October 2016, 189-194, 2016.

Ke, M., Zhu, B., Zhao, J., Deng, W.: Integrated positioning method for intelligent vehicle based on GPS and UWB, SAE Int. J. Passeng. Cars – Electron. Electr. Syst., 11, 40-47, https://doi.org/10.4271/07-11-01-0004, 2017.

Khajenasiri, I., Zhu, P., Verhelst, M., Gielen, G.: Low-energy UWB transceiver implementation for smart home energy management, in: The 18th IEEE International Symposium on Consumer Electronics (ISCE 2014), JeJu Island, South Korea, 22-25 June 2014, 1-2, 2014

Kim, E., Choi, D.: A UWB positioning network enabling unmanned aircraft systems auto land, Aerosp. Sci. Technol., 58, 418-426, https://doi.org/10.1016/j.ast.2016.09.005, 2016.

Kolakowski, M.: Kalman filter based localization in hybrid BLE-UWB positioning system, in: 2017 IEEE International Conference on RFID Technology & Application (RFID-TA), Warsaw, Poland, 20-22 September 2017, 290-293, 2017.

Ledergerber, A., Hamer, M., D'Andrea, R.: A robot self-localization system using one-way ultra-wideband communication, in: 2015 IEEE/RSJ International Conference on Intelligent Robots and Systems (IROS), Hamburg, Germany, 28 September-2 October 2015, 3131-3137, 2015

Madany, Y. M., Elaziz, D. A., Elkrim, W. A.: Design and analyis of compact ultra-wideband inverted FL microstrip patch antenna for intelligent transportation communication systems, in: 2012 15 International Symposium on Antenna Technology and Applied Electromagnetics, Toulouse, France, 25-28 June 2012, 1-4, 2012.

Mokhtari, G., Zhang, Q., Fazlollahi, A.: Non-wearable UWB sensor to detect falls in smart home environment, in: 2017 IEEE International Conference on Pervasive Computing and Communications Workshops (PerCom Workshops), Kona, HI, USA, 13-17 March 2017, 274-278, 2017.

Mostajeran, A., Naghavi, S. M., Emadi, M., Samala, S., Ginsburg, B. P., Aseeri, M., Afshari, E.: A high-resolution 220-GHz ultra-wideband fully integrated ISAR imaging system, IEEE Trans. Microw. Theory Tech., 67, 429-442, https://doi.org/10.1109/TMTT.2018.2874666, 2018.

https://doi.org/10.5194/gi-2019-42
Preprint. Discussion started: 22 June 2020
© Author(s) 2020. CC BY 4.0 License.

Geoscientific Instrumentation Methods and Data Systems Discussions

Nakamura, A., Shimada, N., Itami, M.: Performance analysis of UWB positioning system at the crossing, in: 2018 21st International Conference on Intelligent Transportation Systems (ITSC), Maui, HI, USA, 4-7 November. 2018, 786-791, 2018.

Perez-Grau, F. J., Caballero, F., Merino, L., Viguria, A.: Multi-modal mapping and localization of unmanned aerial robots based on ultra-wideband and RGB-D sensing, in: 2017 IEEE/RSJ International Conference on Intelligent Robots and Systems (IROS), Vancouver, BC, Canada, 24-28 September 2017, 3495-3502, 2017.

Ruiz, A. R., Granja, F. S.: Comparing Ubisense, BeSpoon, and DecaWave UWB location systems: Indoor performance analysis, IEEE Trans. Instrum. Meas., 66, 2106-2117, https://doi.org/10.1109/TIM.2017.2681398, 2017.

Schroeer, G.: A real-time UWB multi-channel indoor positioning system for industrial scenarios, in: 2018 International Conference on Indoor Positioning and Indoor Navigation (IPIN), Nantes, France, 24-27 September 2018, 1-5, 2018.

Stampa, M., Mueller, M., Hess, D., Roehrig, C.: Semi-automatic calibration of UWB range measurements for an autonomous mobile robot, in: ISR 2018; 50th International Symposium on Robotics, Munich, Germany, 20-21 June 2018, 1-6, 2018.

Wang, K.: Application of UWB technology in the development of football training load monitoring system, Int. J. Simul. Syst. Sci. Technol., 16, 8.1-8.6, https://doi.org/10.5013/IJSSST.a.16.3B.08, 2015.

Zhang, H., Zhang, Y., Wang, F.: UWB radar imaging of multiple targets through multi-layer walls, Int. J. Hybrid Inf. Technol., 9, 315-322, https://doi.org/10.14257/ijhit.2016.9.8.27, 2016.

https://doi.org/10.5194/gi-2019-42
Preprint. Discussion started: 22 June 2020
© Author(s) 2020. CC BY 4.0 License.

Geoscientific Instrumentation Methods and Data Systems Discussions
Open Access
EGU

Table 1 Expectation and standard deviation of distance measurements.

Truth value (mm)	Expectations value (mm)	standard deviation (mm)
3560	3810	48.19
9640	9633	58.41
28220	28719	37.80
41540	41973	96.57

https://doi.org/10.5194/gi-2019-42
Preprint. Discussion started: 22 June 2020
© Author(s) 2020. CC BY 4.0 License.

Geoscientific Instrumentation Methods and Data Systems Discussions

Table 2 Truth value, (measured) peak value, and (measured) mean value of the 50 training data sets.

Truth value (m)	Peak value (m)	Mean value (m)
0.6	0.707	0.705
1.2	1.25	1.247
1.8	1.892	1.894
2.4	2.512	2.5
3	3.085	3.098
3.6	3.723	3.588
4.8	4.882	4.892
5.4	5.492	5.332
6	6.118	5.852
6.6	6.684	6.88
7.2	8.514	8.368
7.8	7.911	7.317
8.4	8.461	8.543
9.6	10.514	9.741
10.2	11.061	10.851
10.8	10.851	10.415
11.4	13.219	12.007
12	12.403	12.401
12.6	13.468	12.954
13.2	13.32	13.241
13.8	13.999	13.878
15	15.417	14.658
15.6	16.025	16.043
16.2	16.474	15.667
16.8	16.773	16.155
17.4	17.4	17.009
18.6	18.862	18.009
19.2	19.274	18.271
19.8	20.396	19.315
21	20.97	20.375
21.6	21.706	21.139
22.2	22.389	21.625
23.4	23.377	22.867
24	24.557	24.095
24.6	25.134	24.818
25.2	25.894	25.648
25.8	26.512	26.484
26.4	27.172	27.147
27.6	28.258	28.243
28.2	28.738	28.719
28.8	29.507	29.473
29.4	29.924	29.938
30	30.473	30.247
31.2	31.9	31.897
31.8	32.522	32.519
32.4	33.116	33.097
33	33.705	33.693
34.2	34.889	34.884
34.8	35.477	35.472
36	36.634	36.568

https://doi.org/10.5194/gi-2019-42
Preprint. Discussion started: 22 June 2020
© Author(s) 2020. CC BY 4.0 License.

Geoscientific Instrumentation Methods and Data Systems Discussions
Open Access
EGU

225 **Table 3** Results of true value estimation for 10 sets of test data.

Truth value (m)	Peak value (m)	Expectations value (m)	Estimated value (m)
4.2	4.321	4.29	4.096774
9	9.01	8.318	8.719659
14.4	14.585	14.331	14.21605
18	17.989	17.576	17.57206
20.4	20.487	19.898	20.03483
22.8	23.593	23.197	23.09704
27	27.667	27.542	27.1136
30.6	31.152	31.149	30.54946
33.6	34.314	34.293	33.66687
35.4	36.039	36.044	35.36755

https://doi.org/10.5194/gi-2019-42
Preprint. Discussion started: 22 June 2020
© Author(s) 2020. CC BY 4.0 License.

Geoscientific Instrumentation Methods and Data Systems Discussions
Open Access
EGU

Table 4 Overall estimation error.

Peak estimation error (m)	Expected estimation error (m)	This method estimates the error (m)
0.3779	0.4592	0.1921

https://doi.org/10.5194/gi-2019-42
Preprint. Discussion started: 22 June 2020
© Author(s) 2020. CC BY 4.0 License.

Geoscientific Instrumentation Methods and Data Systems Discussions

Figure captions

Figure 1 Framework of 3D indoor positioning system.

Figure 2 Schematic diagram of the target location results to be measured.

Figure 3 Histogram of the measured values at different distances. (a) Histogram of the measured value at 3560mm. (b) Histogram of the measured value at 9640mm. (c) Histogram of the measured value at 28220mm. (d) Histogram of the measured value at 41540mm.

Figure 4 Fitting results of the probability density distribution curve. (a) Probability density at 3560mm. (b) Probability density at 9640mm. (c) Probability density at 28200mm. (d) Probability density at 41540mm.

Figure 5 Statistical and probability density fitting results of measured values with small data volume. (a) Probability density at 3600mm. (b) Probability density at 11400mm. (c) Probability density at 19200mm. (d) Probability density at 31800mm.

Figure 6 Statistical results and fitting of the peak and true values of distance measurement.

Figure 7 Statistical results after removing abnormal value. (a) The result of rejecting abnormal value at 3600mm. (b) The result of rejecting abnormal value at 11400mm. (c) The result of rejecting abnormal value at 19200mm. (d) The result of rejecting abnormal value at 31800mm.

https://doi.org/10.5194/gi-2019-42
Preprint. Discussion started: 22 June 2020
© Author(s) 2020. CC BY 4.0 License.

Geoscientific Instrumentation Methods and Data Systems Discussions
Open Access
EGU

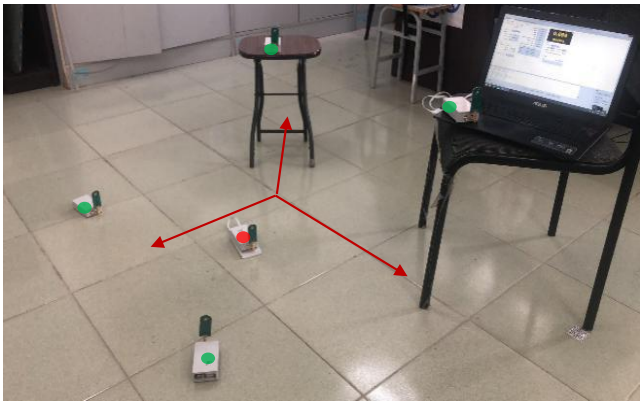

Fig. 1 Framework of 3D indoor positioning system

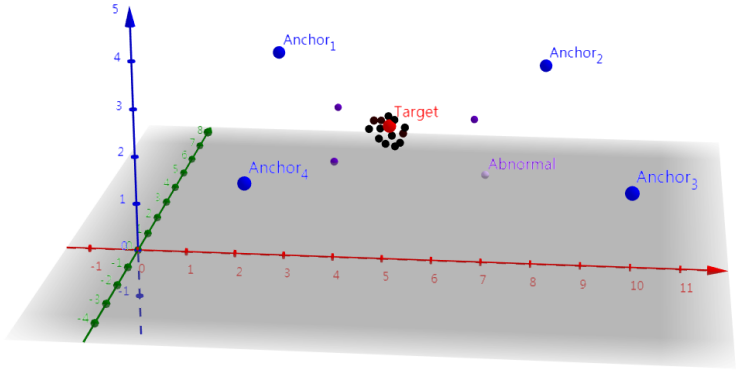

Fig. 2 Schematic diagram of target location results to be measured

https://doi.org/10.5194/gi-2019-42
Preprint. Discussion started: 22 June 2020
© Author(s) 2020. CC BY 4.0 License.

Geoscientific Instrumentation Methods and Data Systems Discussions
Open Access
EGU

(a)

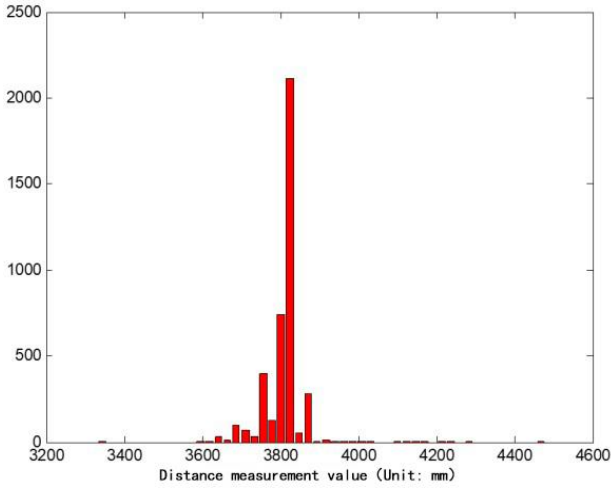

(b)

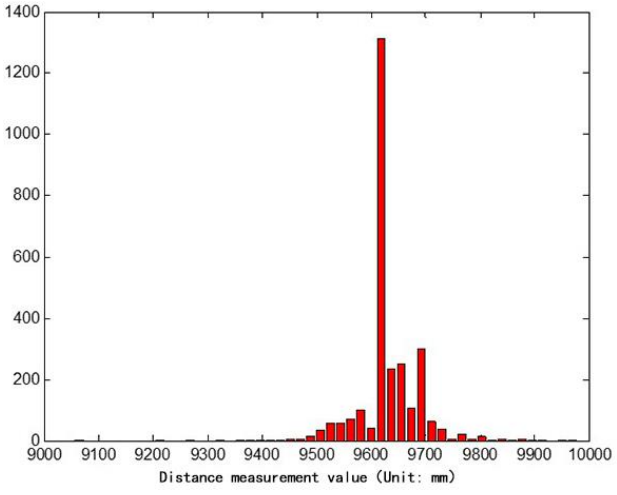

https://doi.org/10.5194/gi-2019-42
Preprint. Discussion started: 22 June 2020
© Author(s) 2020. CC BY 4.0 License.

Geoscientific Instrumentation Methods and Data Systems Discussions

(c)

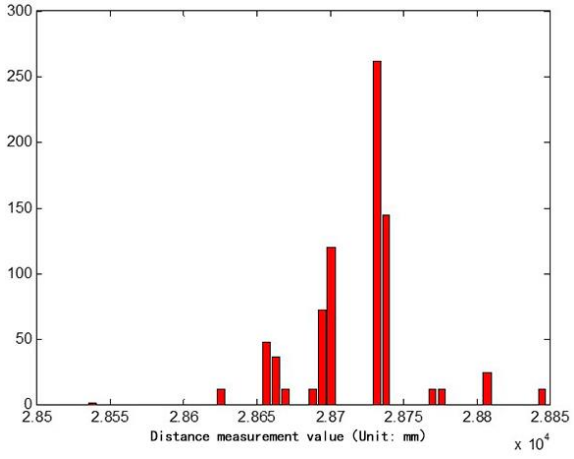

(d)

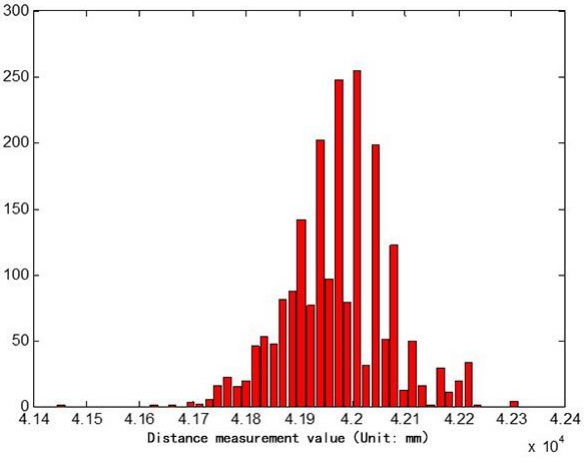

Fig.3 Histogram of the measured values at different distances. (a) Histogram of the measured value at 3560mm. (b) Histogram of the measured value at 9640mm. (c) Histogram of the measured value at 28220mm. (d) Histogram of the measured value at 41540mm.

https://doi.org/10.5194/gi-2019-42
Preprint. Discussion started: 22 June 2020
© Author(s) 2020. CC BY 4.0 License.

Geoscientific Instrumentation Methods and Data Systems Discussions
Open Access
EGU

(a)

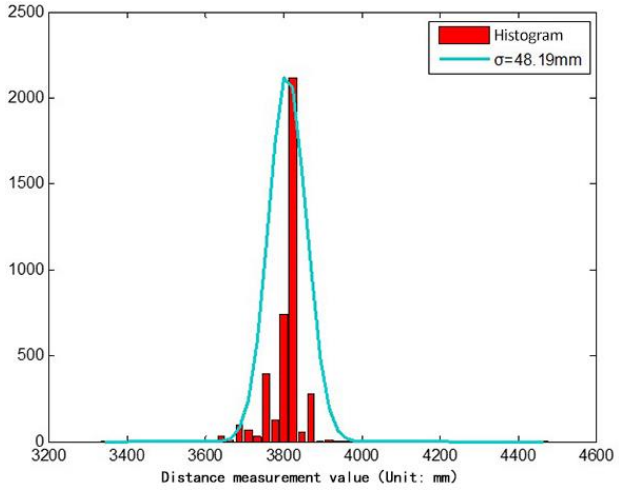

(b)

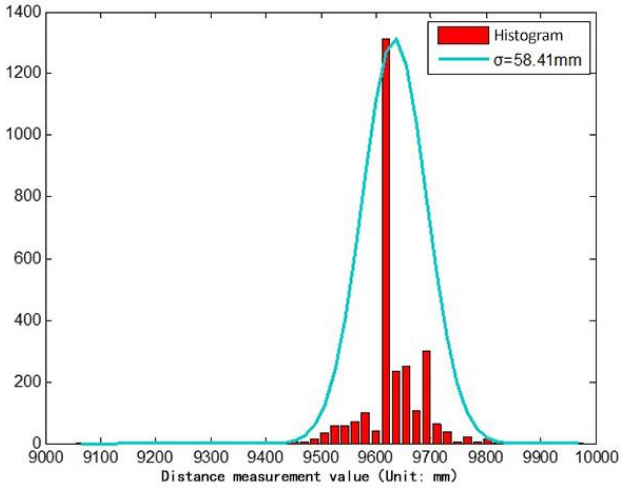

https://doi.org/10.5194/gi-2019-42
Preprint. Discussion started: 22 June 2020
© Author(s) 2020. CC BY 4.0 License.

Geoscientific Instrumentation Methods and Data Systems Discussions
Open Access
EGU

(c)

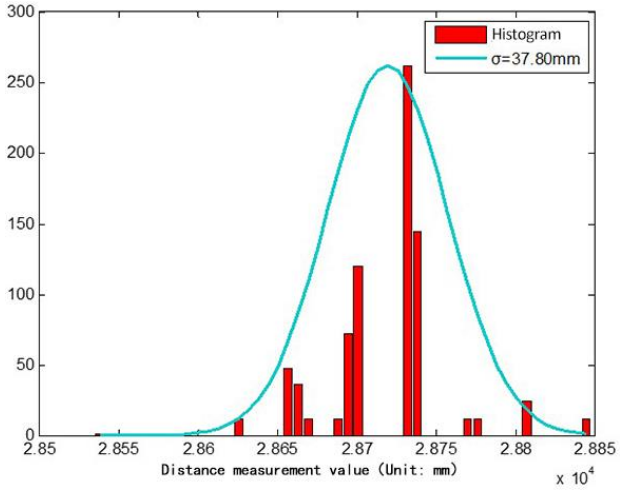

(d)

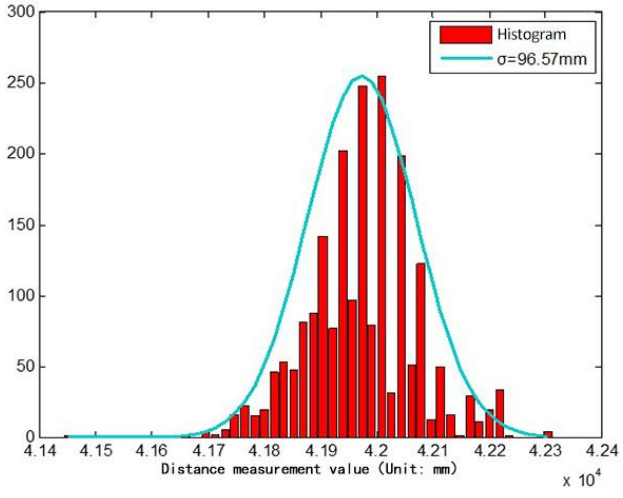

Fig.4 Fitting results of the probability density distribution curve. (a) Probability density at 3560mm. (b) Probability density at 9640mm. (c) Probability density at 28200mm. (d) Probability density at 41540mm.

https://doi.org/10.5194/gi-2019-42
Preprint. Discussion started: 22 June 2020
© Author(s) 2020. CC BY 4.0 License.

Geoscientific Instrumentation Methods and Data Systems Discussions
Open Access
EGU

(a)

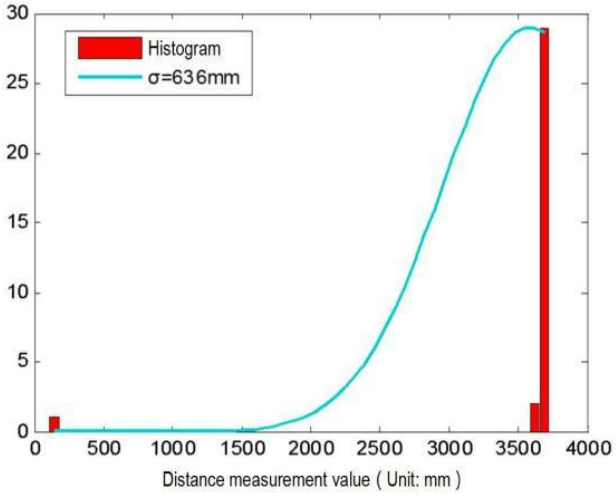

(b)

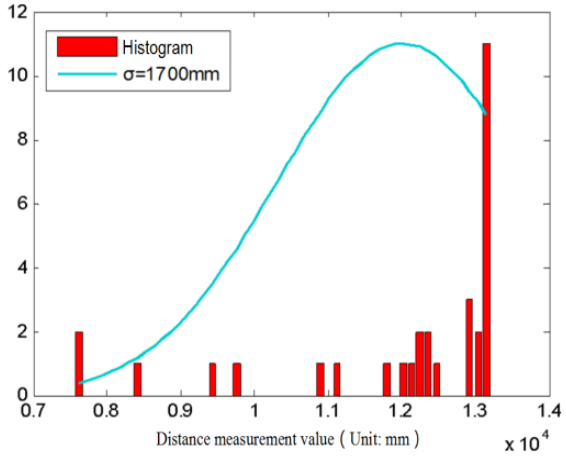

https://doi.org/10.5194/gi-2019-42
Preprint. Discussion started: 22 June 2020
© Author(s) 2020. CC BY 4.0 License.

Geoscientific Instrumentation Methods and Data Systems Discussions
Open Access
EGU

(c)

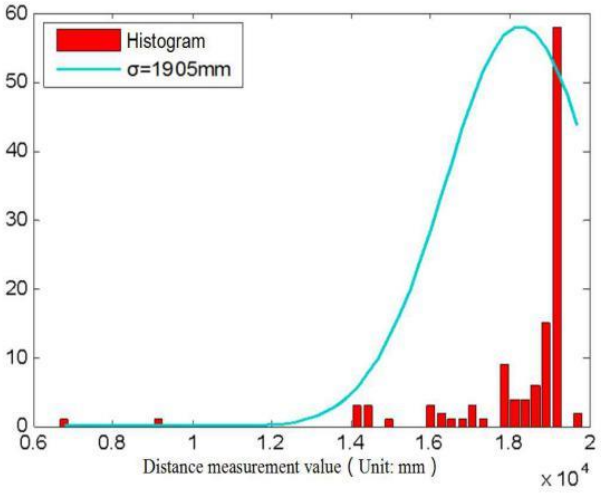

(d)

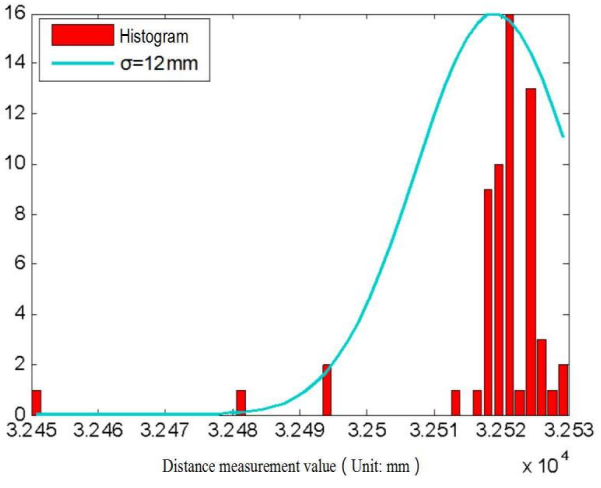

Fig.5 Statistical and probability density fitting results of measured values with small data volume. (a) Probability density at 3600mm. (b) Probability density at 11400mm. (c) Probability density at 19200mm. (d) Probability density at 31800mm.

https://doi.org/10.5194/gi-2019-42
Preprint. Discussion started: 22 June 2020
© Author(s) 2020. CC BY 4.0 License.

Geoscientific Instrumentation Methods and Data Systems Discussions
Open Access
EGU

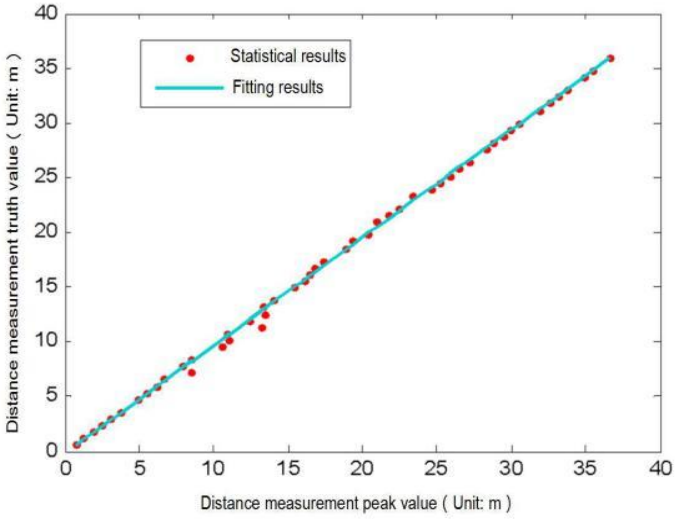

Fig.6 Statistical and fitting results of peak value and truth value of distance measurement

https://doi.org/10.5194/gi-2019-42
Preprint. Discussion started: 22 June 2020
© Author(s) 2020. CC BY 4.0 License.

Geoscientific Instrumentation Methods and Data Systems Discussions
Open Access
EGU

(a)

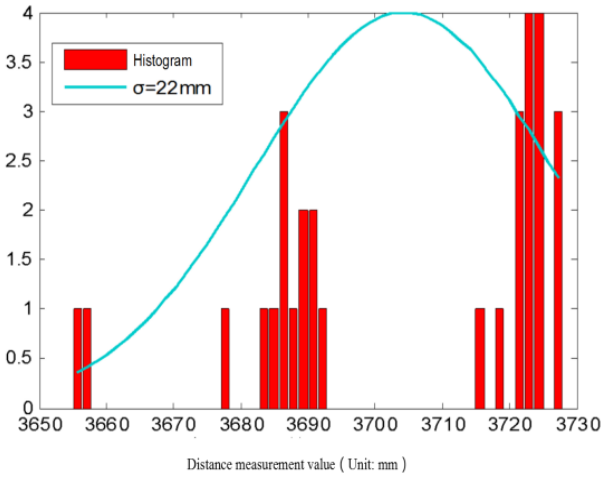

(b)

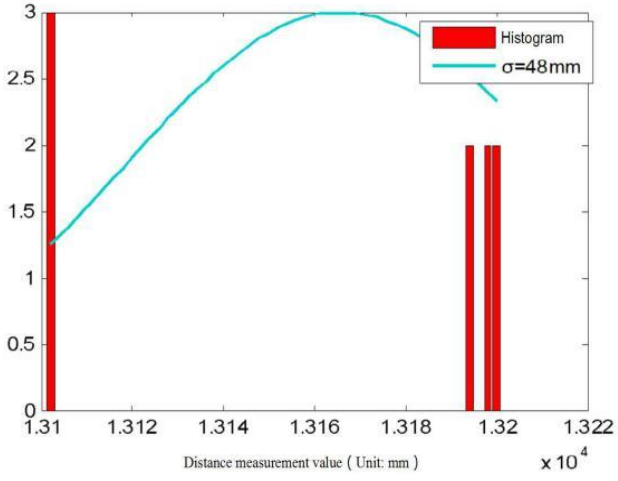

https://doi.org/10.5194/gi-2019-42
Preprint. Discussion started: 22 June 2020
© Author(s) 2020. CC BY 4.0 License.

Geoscientific Instrumentation Methods and Data Systems Discussions
Open Access
EGU

(c)

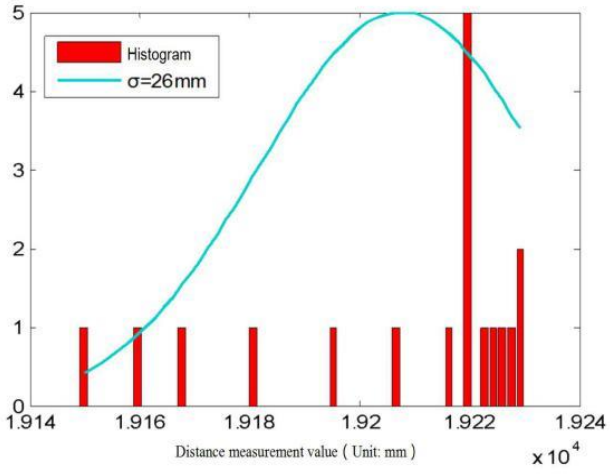

(d)

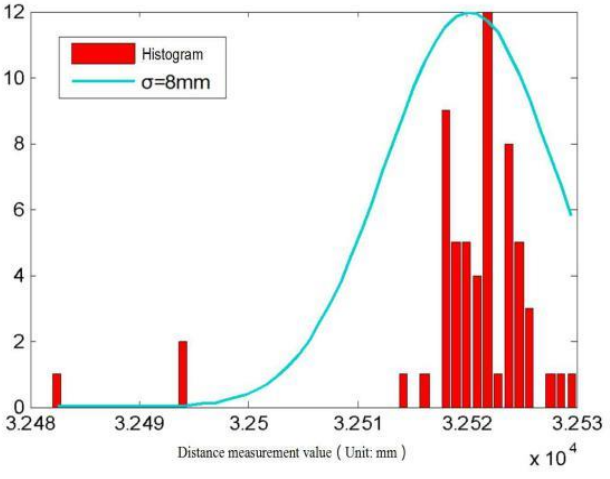

Fig.7 Statistical results after removing abnormal value. (a) The result of rejecting abnormal value at 3600mm. (b) The result of rejecting abnormal value at 11400mm. (c) The result of rejecting abnormal value at 19200mm. (d) The result of rejecting abnormal value at 31800mm.